

PRECLINICAL RESEARCH

MLb-LDLr

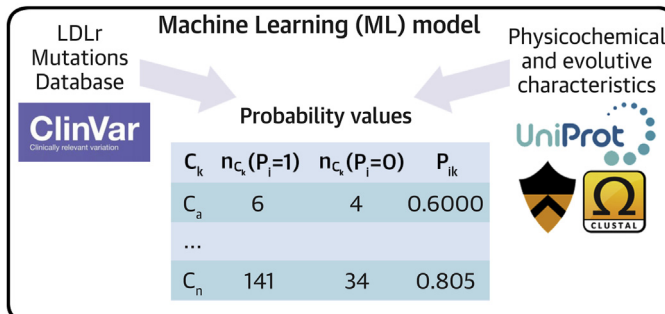
A Machine Learning Model for Predicting the Pathogenicity of *LDLr* Missense Variants



Asier Larrea-Sebal, MSc,^{a,b} Asier Benito-Vicente, PhD,^{b,c} José A. Fernandez-Higuero, PhD,^c
Shifa Jebari-Benslaïman, MSc,^{b,c} Unai Galicia-Garcia, PhD,^{a,b} Kepa B. Uribe, PhD,^d Ana Cenarro, PhD,^e
Helena Ostolaza, PhD,^{b,c} Fernando Civeira, MD, PhD,^e Sonia Arrasate, PhD,^f Humberto González-Díaz, PhD,^{b,g}
César Martín, PhD^{b,c}

VISUAL ABSTRACT

80 benign and 664 pathogenic LDL receptor (LDLr) variants identified from NCBI ClinVar database and the literature



Results
ML model (MLb-LDLr) has been developed
92% sensitivity
91.5% specificity

Larrea-Sebal, A. et al. J Am Coll Cardiol Basic Trans Science. 2021;6(11):815-827.

HIGHLIGHTS

- A machine-learning model has been developed to improve accuracy on predicting the activity of missense *LDLr* mutations.
- ClinVar was used as database, and the model function was defined by using specific characteristics of the *LDLr*.
- A high-score prediction ML model with specificity of 92.5% and sensitivity of 91.6% has been developed to predict pathogenicity of *LDLr* variants.
- Implementation of high-predicting capacity software constitutes a valuable approach for assessing pathogenicity of *LDLr* variants to help in the early diagnosis and management of FH disease.
- An open-access predictive software (MLb-LDLr) is provided to the scientific community.

From the ^aFundación Biofísica Bizkaia, Leioa, Spain; ^bInstituto Biofísica (UPV/EHU, CSIC), University of the Basque Country, Leioa, Spain; ^cDepartment of Biochemistry and Molecular Biology, University of the Basque Country, Leioa, Spain; ^dCenter for Cooperative Research in Biomaterials (CIC biomAGUNE), Basque Research and Technology Alliance (BRTA), Donostia San Sebastián, Spain; ^eLipid Unit, Hospital Universitario Miguel Servet, IIS Aragón, CIBERCV, Universidad de Zaragoza, Spain; ^fDepartment of Organic and Inorganic Chemistry, University of Basque Country UPV/EHU, Leioa, Spain; and the ^gIKERBASQUE, Basque Foundation for Science, Bilbao, Spain.

**ABBREVIATIONS
AND ACRONYMS****ANN** = artificial neural network**AUROC** = area under the receiver operating curve**EGS** = expert-guided selection**ESEA** = Excel Solver Evolutionary algorithm**FH** = familial hypercholesterolemia**LDA** = linear discriminant analysis**LDL** = low-density lipoprotein**LDLr** = low-density lipoprotein receptor**LNN** = linear neural networks**ML** = machine learning**MLb-LDLr** = machine-learning-based low-density lipoprotein receptor software**MLP** = multilayer perceptron**RBF** = radial basis function**UTR** = untranslated region**SUMMARY**

Untreated familial hypercholesterolemia (FH) leads to atherosclerosis and early cardiovascular disease. Mutations in the low-density lipoprotein receptor (*LDLr*) gene constitute the major cause of FH, and the high number of mutations already described in the *LDLr* makes necessary cascade screening or in vitro functional characterization to provide a definitive diagnosis. Implementation of high-predicting capacity software constitutes a valuable approach for assessing pathogenicity of *LDLr* variants to help in the early diagnosis and management of FH disease. This work provides a reliable machine learning model to accurately predict the pathogenicity of *LDLr* missense variants with specificity of 92.5% and sensitivity of 91.6%.

(J Am Coll Cardiol Basic Trans Science 2021;6:815-827) © 2021 The Authors. Published by Elsevier on behalf of the American College of Cardiology Foundation. This is an open access article under the CC BY-NC-ND license (<http://creativecommons.org/licenses/by-nc-nd/4.0/>).

Familial hypercholesterolemia (FH) is the most common autosomal dominant disorder with an estimated prevalence between 1:200 and 1:250 (1). FH is characterized by an elevated concentration of low-density lipoprotein (LDL) cholesterol in plasma as a consequence of a defective catabolism of LDL particles (2). The progression of FH is asymptomatic and normally is

not detected until advanced stages of the disease when long-term exposure to LDL induces the development of atheroma plaques and increases the risk of cardiovascular diseases (3,4). Despite the high incidence of FH, <1% of the patients are properly diagnosed, and consequently, the implementation of early intervention programs to prevent plasma LDL accumulation and long-term associated problems is limited (5,6).

Mutations in the LDL receptor gene (*LDLr*) are the most common genetic cause of FH, accounting for more than 90% of the cases (7). To date, more than 3,000 *LDLr* genetic variants have been described and submitted to the ClinVar database. Among them, missense variants, resulting from single nucleotide substitution, are the most frequent ones (8). Single nucleotide variations can affect (pathogenic) or not (benign) protein structure and function; however, only a reduced number of variants have been functionally validated and proven to be pathogenic (9). Cascade screening and in vitro functional characterization are the most reliable methodologies to validate pathogenicity of *LDLr* variants (10). Nevertheless, both methods have their own limitations: in vitro functional validation is laborious and

time-consuming, whereas cascade screening requires patient clinical data availability and a high number of patients (11). Lately, the use of computational tools has been extended to many fields of medical sciences, including development of predictive software to assess the pathogenicity of protein variants (12,13). Given the high frequency of the mutations found in the *LDLr* gene, developing specific software to predict *LDLr* pathogenicity would allow a rapid and systematic characterization of pathogenic variants.

Taking advantage of the large number of missense *LDLr* variants already characterized and annotated in the ClinVar database, the aim of this work has been to develop an advanced machine learning (ML) algorithm to accurately predict the pathogenicity of *LDLr* missense variants. To do so, 7 characteristics of the protein have been considered in order to obtain a high-score prediction. The introduction of a ML algorithm provides a predictive model with a specificity of 92.5% and a sensitivity of 91.6%, which shows high accuracy in predicting both pathogenic and benign variants. Here, we provide an open access machine learning-based *LDLr* predictive software (MLb-*LDLr*) for the scientific community to predict the pathogenicity of missense *LDLr* variants (14). Ultimately, the data presented here will help clinicians and researchers interpret the effect of any missense mutation in the *LDLr* gene.

METHODS

DATASET. To date, more than 3,000 *LDLr* variants have been annotated in the ClinVar database (May 25, 2021). These variants are divided into 6 subclasses

The authors attest they are in compliance with human studies committees and animal welfare regulations of the authors' institutions and Food and Drug Administration guidelines, including patient consent where appropriate. For more information, visit the [Author Center](#).

Manuscript received June 1, 2021; revised manuscript received August 26, 2021, accepted August 28, 2021.

according to the type of the mutation: frameshift, missense, nonsense, splice site, noncoding RNA, and untranslated region (UTR). In order to develop an efficient ML diagnostic tool, each subclass must be analyzed individually because a given feature could be important for one subclass, but not relevant for others, taking into account their very different effect. However, most of the subclasses have a reduced number of variants, thus prediction of protein activity is not possible due to the limited available information. In addition to limited data availability, the nature of some mutation subclasses leads to a deleterious effect in most of the variants (ie, frameshift and nonsense mutations) or almost always a benign effect (noncoding RNA and UTR). Therefore, the lack of enough variants with the contrary effect does not allow obtaining an accurate ML model if included. On the other hand, the existence of large amount of both pathogenic and benign *LDLR* missense variants whose activity has been validated allows the development of a ML predictive software to predict the pathogenicity of these variants.

More than 1,200 missense variants are already annotated in ClinVar, which are distributed according to their pathogenicity as follows: 7 benign, 58 likely benign, 284 of uncertain significance, 239 of conflictive interpretation, 568 likely pathogenic, and 248 pathogenic, although some of these variants have been included into more than 1 subclass. In order to ease the classification, benign and likely benign variants were grouped into a benign subclass (n = 65), and pathogenic and likely pathogenic variants into a pathogenic subclass (n = 639). ClinVar is a great source to evaluate the pathogenicity of *LDLR* variants, and although most of the used variants have multiple submitters to support their pathogenicity, 1 limitation of the database is that in some cases, there is only 1 submitter, and a few of them have no assertion. Therefore, this has been taken into consideration in the training and validation of the model.

In addition, an exhaustive bibliographic search allowed to ascertaining the effect of variants with conflictive interpretation or uncertain significance and their inclusion in the benign or pathogenic categories. This process allowed increasing the number of variants with a reliable diagnosis. In sum, the data set consisted of 80 benign and 664 pathogenic *LDLR* variants.

MODEL DEFINITION. A classification model to predict the probability $p(P_i = 1)_{pred}$ of pathogenicity (P_i) of the i^{th} protein variant was defined. Applying these criteria, the model fits the objective function $f(P_i)_{obs}$. The function $f(P_i)_{obs} = 1$ when $P_i =$ pathogenic and

$f(P_i)_{obs} = 0$ when $P_i =$ benign. The output of the model is the scoring function $f(P_i)_{calc}$. This function gets real values and consequently cannot be compared directly to $f(P_i)_{obs}$. As a consequence, $f(P_i)_{calc}$ was transformed into the searched probability scale values $p(P_i = 1)_{pred}$. Using these probability values, the predicted classification of each protein variant $f(P_i)_{pred}$ can be obtained. The predicted classification $f(P_i)_{pred} = 1$ ($P_i =$ pathogenic) when $p(P_i = 1)_{pred} > 0$, otherwise $f(P_i)_{pred} = 0$ ($P_i =$ benign). Both linear and nonlinear ML models were trained. The general formula for the linear ML model is shown in Equation 1.

$$f(P_i)_{calc} = -e_0 + \sum_{k=1}^{k=7} e_k \cdot P_{ik} \quad (1)$$

The coefficient e_0 is the independent term, and $e_{k>0}$ are the coefficients for each input variable P_{ik} . These coefficients $e_{k>0}$ quantify the influence (weight) given to each characteristic on the overall pathogenicity. In order to fit the objective function $f(P_i)_{obs}$, we used as input variable P_{ik} parameters. These P_{ik} parameters are the probabilities with which pathogenic protein variants in the data set present a given value of the characteristic C_k within a given range. We encoded P_{ik} values of each protein variant into the quantitative vector $P_{ik} = [P_{i1}, P_{i2}, P_{i3}, \dots, P_{i7}]$. The specific characteristics studied were: $C_1 =$ conservation of the substituted residue, $C_2 =$ charge change, $C_3 =$ original amino acid, $C_4 =$ substituting amino acid, $C_5 =$ amino acid hydrophobicity change, $C_6 =$ amino acid size change, and $C_7 =$ affected domain. These characteristics were further divided into 2 different subgroups: physicochemical ($C_2, C_5, C_6,$ and C_7) or biological-evolutionary ($C_1, C_3,$ and C_4). The values of each characteristic C_k of the 3 continuous variables ($C_1, C_5,$ and C_6) were split into 5 mutually exclusive and equal intervals or classes (c). On the other hand, the values of each characteristic C_k of the discrete variables ($C_2, C_3, C_4,$ and C_7) were split into different classes. Characteristic selection and obtention process are shown in the [Supplemental Appendix and Supplemental Tables S1 to S4](#). C_k variables were transformed into P_{ik} probability values according to Equation 2.

$$P_{ik} = \frac{nC_k(P_i = 1)}{nC_k(P_i = 1) + nC_k(P_i = 0)} \quad (2)$$

In Equation 2, $nC_k(P_i = 1)$ is the number of pathogenic protein variants ($P_i = 1$) with values of C_k within the class c. By analogy, in this formula, $nC_k(P_i = 0)$ is the number of benign protein variants ($P_i = 0$) with values of C_k within the class c. P_{ik} values are shown in [Supplemental Table S5](#).

MODEL TRAINING AND VALIDATION. As mentioned before, training was performed in both linear and nonlinear models. In the case of the ML linear models, different algorithms were used to define the e_k coefficients. The linear ML algorithms used were linear discriminant analysis (LDA) (parametric), linear neural networks (LNN) (nonparametric) from STATISTICA data analysis software system, version 6.0 (StatSoft, Inc.) and Excel Solver Evolutionary algorithm (ESEA) (parametric) (15). In the case of nonlinear models, 2 types of nonlinear artificial neural network (ANN) algorithms were used: multilayer perceptron (MLP) (parametric) and radial basis function (RBF) (nonparametric) (STATISTICA, data analysis software system, version 6.0, StatSoft, Inc.). These models were chosen because they allow testing different types of ML mechanisms, linear and nonlinear, parametric and nonparametric. Linear and parametric models create lineal equations formed by coefficients such as weight or threshold, whereas the nonparametric ones are more complex and use other types of equations.

In order to train/validate the model, the dataset was split into 2 subsets using the variable subset = T (training series) and subset = V (validation series). Variants in training series were used to obtain P_{ik} values and to train the ML models. Variants in validation series were used neither to obtain P_{ik} values nor to train the model. The variants were assigned to training or validation series randomly. Three-quarters of the pathogenic variants ($n = 499$) were used for training and the remaining ($n = 166$) to validate the model. In the case of benign variants, two-thirds ($n = 54$) were used in the training group, and the remaining ($n = 26$) were used in the validation group due to the limited number of annotated variants.

VARIABLE SELECTION AND OPTIMIZATION. In a first stage, linear and ANN ML algorithms from STATISTICA were run with different variable selection strategies: forward stepwise, backward stepwise, etc. Next, ESEA strategy was used. ESEA maximized $f(P_i)_{calc}$ function and increased the number of correctly predicted variants, modifying e_k coefficients (see the details in the Supplemental Appendix). The maximum and minimum limits established for weights and threshold were $e_{k>0max} = 0.2$ and $e_{k>0min} = 0.001$, and $e_{0max} = 1$ and $e_{0min} = 0.1$, respectively. These limit values were set up arbitrarily. In order to obtain a balanced relation between the correctly predicted pathogenic and benign variants, the objective function Equation 3 was described as follows:

$$F_0 = Sensitivity * Specificity \quad (3)$$

Next, ESEA expert-guided selection (EGS) strategy was used to optimize e_k values. EGS was carried out

as follows: Once the best fitting weights and threshold were established through ESEA, some P_{ik} values were adjusted to improve the number of correctly predicted variants. Consequently, EGS strategy included a reparameterization of some P_{ik} values, thus increasing the number of correct predictions; see the details in the Supplemental Appendix and Supplemental Table S6. The general workflow of the model is shown in Figure 1.

STATISTICAL ANALYSIS. Accuracy of the model was tested by 4 statistic parameters: sensitivity, specificity, positive predictive value, and negative predictive value. The sensitivity and the specificity values refer to the percentage of correctly predicted pathogenic and benign variants, respectively. These parameters were calculated in both training and validation sets.

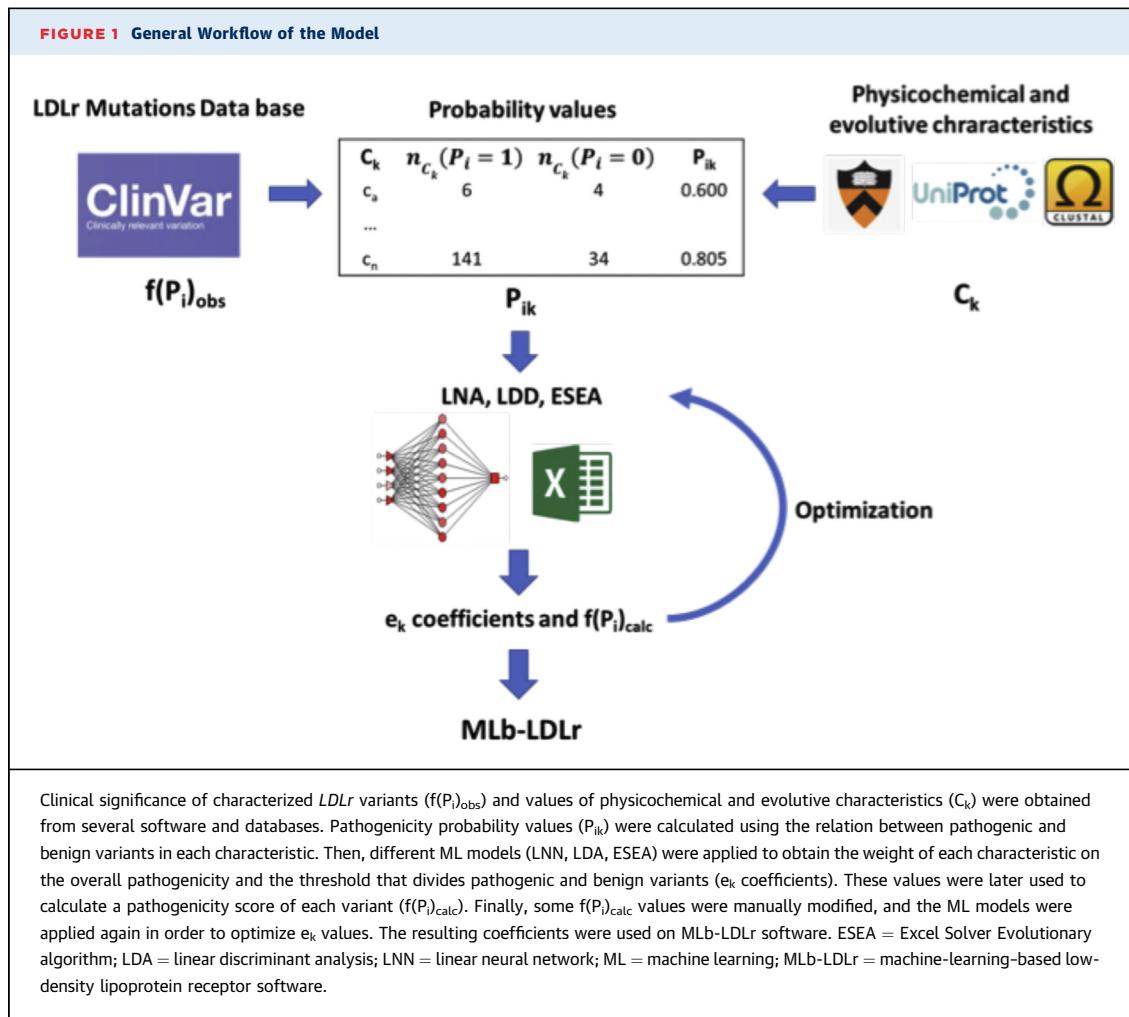
In addition, random bootstrapping training and validation subsets of the same sample size with replacement were used to test the sampling distribution. One thousand bootstrapped samples were tested, and the statistics previously mentioned were presented with 95% confidence intervals.

EXPERIMENTAL MODEL VALIDATION. In vitro functional characterization of ClinVar-annotated conflictive *LDLr* variants.

***LDLr* VARIANT SELECTION.** Thirteen *LDLr* variants with conflictive or uncertain interpretations on ClinVar were selected to experimentally validate the accuracy of MLb-*LDLr* and other predictive software. The selection criteria were based on the disparity of the prediction of the most used pathogenicity-predictive software. Hence, not only the functional characterization of conflictive *LDLr* variants was performed, but also software accuracy was assessed when facing a hard to predict variant. In addition, the selected variants have been described in patients with elevated levels of LDL cholesterol. Descriptions of the studied variants and in silico predictions are shown in Table 1.

CHO-*ldlΔ7* CELL CULTURE AND TRANSFECTION.

The CHO-*ldlΔ7* cell line was cultured in Dulbeccó's modified eagle medium low glucose, 1 g/L (GE Healthcare) supplemented with 10% fetal bovine serum, 2 mmol/L L-glutamine, 100 units/mL penicillin, and 100 μg/mL streptomycin. Ten thousand CHO-*ldlΔ7* cells were plated into 96-well culture plates and transiently transfected with the plasmids carrying wild-type *LDLr* or Ex3_4del, c.599T>G p.(Phe200Cys), c.889A>C p.(Asn297His), c.914G>C p.(Trp305Ser), c.1112T>C p.(Lau371Pro), c.1118G>C p.(Gly373Ala), 1345A>G p.(Arg449Gly), c.1418T>A p.(Ile473Asn), 1732G>A p.(Val578Ile), 1912G>C p.(Asp638His),



c.1955T>C p.(Met652Thr), c.2049C>T p.(Pro683Leu), c.2098G>A p.(Asp700Asn), and c.2113G>C p.(Ala705Pro) *LDLr* variants using Lipofectamine 2000 Transfection Reagent (Thermo Fisher Scientific). Transfected cells were maintained in culture for 48 hours to achieve maximal *LDLr* expression.

QUANTIFICATION OF *LDLr* ACTIVITY. *LDLr* activity was determined by flow cytometry in CHO-*ldlΔ7* cells transfected with plasmids encoding the *LDLr* variants as previously described (16). Transfected CHO-*ldlΔ7* cells were grown in 96-well culture plates. Forty-eight hours after transfection, cells were incubated 4 hours at 37 °C with 20 μg/mL fluorescein isothiocyanate-LDL. Cells were then washed twice in phosphate-buffered saline and incubated with phosphate-buffered saline 5% EDTA for 10 min. To determine the amount of internalized LDL, Trypan blue solution (Sigma-Aldrich) was added directly to the samples to a final concentration of 0.2% (v/v) to extinguish the extracellular signal by dynamic quenching of the noninternalized LDLr-LDL

complexes (17). Fluorescence intensities were measured by flow cytometry in a CytoFlex cytometer (Beckman Coulter) according to the manufacturer's instructions. For each sample, fluorescence of 10,000 events was acquired for data analysis, and the results were expressed as the mean fluorescence.

ETHICAL APPROVAL. All methods were carried out in accordance with relevant guidelines and regulations. This study was approved by the research ethics committee from the University of the Basque Country (Comité de Ética en la Investigación y la Práctica Docente de la Universidad del País Vasco/Euskal Herriko Unibertsitatea, CEID/IEEB).

RESULTS

COMPUTATIONAL MODEL FOR PATHOGENICITY PREDICTION. Once the weights of each characteristic in the overall pathogenicity ($e_{k>0}$) and the pathogenicity threshold (e_0) were calculated (Supplemental Table S7), pathogenicity prediction of

TABLE 1 Selected *LDLr* Variants for In Vitro Characterization and Their Pathogenicity Prediction

<i>LDLr</i> Variant	MLb-LDLr	PolyPhen-2	SIFT	SFIP-MutID	MutationTaster	CADD
p.(Phe200Cys)	Pathogenic	Pathogenic	Benign	Pathogenic	Pathogenic	Pathogenic
p.(Asn297His)	Pathogenic	Benign	Benign	Pathogenic	Pathogenic	Pathogenic
p.(Trp305Ser)	Pathogenic	Pathogenic	Benign	Pathogenic	Pathogenic	Pathogenic
p.(Leu371Pro)	Pathogenic	Pathogenic	Benign	Pathogenic	Benign	Pathogenic
p.(Gly373Ala)	Pathogenic	Pathogenic	Benign	Benign	Pathogenic	Pathogenic
p.(Arg449Gly)	Pathogenic	Benign	Benign	Pathogenic	Pathogenic	Benign
p.(Ile473Asn)	Benign	Benign	Pathogenic	Pathogenic	Pathogenic	Benign
p.(Val578Ile)	Benign	Pathogenic	Benign	Pathogenic	Benign	Benign
p.(Asp638His)	Pathogenic	Pathogenic	Benign	Pathogenic	Pathogenic	Pathogenic
p.(Met652Thr)	Benign	Benign	Pathogenic	Pathogenic	Pathogenic	Pathogenic
p.(Pro683Leu)	Pathogenic	Pathogenic	Benign	Pathogenic	Benign	Benign
p.(Asp700Asn)	Pathogenic	Pathogenic	Benign	Pathogenic	Pathogenic	Benign
p.(Ala705Pro)	Benign	Benign	Benign	Pathogenic	Pathogenic	Pathogenic

CADD = Combined Annotation-Dependent Depletion software; MLb-LDLr = machine-learning-based low-density lipoprotein receptor software; PolyPhen-2 = Polymorphism Phenotyping v2 software; SFIP-MutID = structure-based functional impact prediction for mutation identification; SIFT = Sorting Intolerant From Tolerant software.

missense *LDLr* variants was assessed following the equation model shown in Equation 4.

$$f(P_i)_{calc} = -(+0.667) + 0.082 \cdot P_{i1} + 0.132 \cdot P_{i2} + 0.093 \cdot P_{i3} + 0.088 \cdot P_{i4} + 0.165 \cdot P_{i5} + 0.115 \cdot P_{i6} + 0.077 \cdot P_{i7} \quad (4)$$

Where $N_{Training} = 552$, $N_{Validation} = 192$, $N_{Total} = 744$, $\chi^2 = 349$, and $P < 0.05$. The model classifies correctly 91.2% of pathogenic variants (454 of 498) and 90.7% of benign variants (49 of 54) on training, and 92.8% of pathogenic (154 of 166) and 96.2% of benign (25 of 26) on validation. The positive predictive values are 98.9% and 99.9% on training and validation, respectively, and negative predictive values are 52.7% and 67.6% on training and validation, respectively.

The obtained results show the predictive ability of the model, which is able to classify *LDLr* variants into benign or pathogenic with an accuracy higher than 90% in training and validation. The similarity between specificity and sensitivity parameters of MLb-LDLr is explained by obtaining the variables through the ESA algorithm, where balance on the percentage of correctly predicted pathogenic and benign variants was prioritized instead of better overall score in only 1 category (Equation 3). However, this process was performed only with training variants, so the balance on validation ones is a sign of the homogeneity of the training/validation data set division.

COMPARATIVE ANALYSIS OF THE PREDICTIVE ACCURACY OF ML-BASED METHODOLOGIES. The predictive accuracy of 5 ML models was tested: 3 linear models (LDA, LNN, and ESEA) and 2 nonlinear ones from ANN (MLP and RBF) (Table 2). LDA shows a

much lower specificity and a slightly higher sensitivity than ESEA. By contrast, MLP, RBF, and LNN show a slightly higher specificity but much lower sensitivity than ESEA.

MLb-LDLr SOFTWARE. The best ML model found with ESEA was implemented into user-friendly software denominated MLb-LDLr. MLb-LDLr was developed using several libraries: Python (3.8.5), Click (7.1.2), Flask (1.1.2), Gunicorn (20.0.4), Itsdangerous (1.1.0), Jinja2 (2.11.2), MarkupSafe (1.1.1), and Werkzeug (1.0.1). The code and the database used for the software are available at GitHub under Creative Commons CC0 license.

MLb-LDLr software uses its own algorithm to give pathogenicity predictions of every single *LDLr* missense variant. $f(P_i)_{calc}$ score values were relativized to a maximum and the pathogenicity threshold. The final percentage value is obtained relativizing the score to 100 (5).

$$p(P_i = X)_{pred} = \begin{cases} f(P_i = 1)_{calc} > e_0, & \frac{f(P_i = 1)_{calc} - e_0}{\text{Max}(f(P_i = 1)_{calc}) - e_0} * 50 + 50 \\ f(P_i = 1)_{calc} < e_0, & -\frac{f(P_i = 1)_{calc} - e_0}{\text{Max}(f(P_i = 1)_{calc}) - e_0} * 50 - 50 \end{cases} \quad (5)$$

The maximum possible value ($\text{Max}(f(P_i = 1)_{calc})$) is obtained when $P_{i1} = P_{i2} = \dots = P_{i7} = 1$ (Equation [4]). The max value gets only positive values because during the ESEA optimization, we used the restriction $e_k > 0$. Because it is not possible for any *LDLr* missense variants to reach that value ($f(P_i=1)_{calc} = 0.752$) using this model, the maximum value was set in

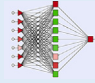
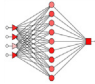
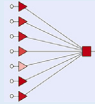
$f(P_1 = 1)_{calc} = 0.74$ in order to obtain more accurate results. The software visualizes the final probability values ($p(P_1 = 1)\%$ or $p(P_1 = 0)\%$) in a 50-100 scale. Whether a variant is predicted as a benign ($f(P_1 = 1)_{calc} < e_0$), the software visualizes $p(P_1 = 0)\%$. This way, the result displayed is always positive and higher than 50% of being pathogenic or benign. The top-5 pathogenic and benign variant predictions on the training and validation groups are shown in Supplemental Table S8. The complete prediction database is shown in Supplemental Table S9, and data used for prediction are available on Figshare.

MLb-LDLr INTERFACE. Both DNA or amino acid nomenclature can be used as input, and the software is able to carry out multiple analyses at once (Figure 2). The result summary includes information about the affected domain, the conservation and amino acid size, charge, and hydrophobicity change. The information of the last 4 characteristics is given in “low,” “medium,” or “high” format (Figure 3), according to Supplemental Table S6 probability table values.

ACCURACY OF MLb-LDLr VERSUS OTHER PREDICTIVE SOFTWARE. To date, several software programs are available to predict the effect of a given mutation on the protein function. Although most of them are used to predict the functional effect of a mutation in any protein (eg, Polymorphism Phenotyping v2 [PolyPhen-2] [18], Sorting Intolerant From Tolerant [SIFT] [19], Combined Annotation-Dependent Depletion [CADD] [20], MutationTaster [21]), recently, a structure-based software for missense *LDLr* variants has been developed (SFIP-MutID) (22). Each model uses different databases and techniques for prediction, so their effectiveness can vary. In this work, we have used all missense *LDLr* variants (744) annotated at ClinVar database to compare the accuracy of different software, with and without bootstrapping resampling. Because EGS optimization process must be done manually, this process has not been carried out on bootstrapped resampling. The main results are shown in Table 3 and Figure 4. The prediction of each variant on the nonbootstrapped sample is shown in Supplemental Table S10.

Regarding the nonbootstrapped samples, MLb-LDLr is the only software program with all statistic values higher than 90%. MutationTaster shows the top score for sensitivity in both training and validation sets but has the second-worst specificity values. The highest specificity in the training set corresponds to MLb-LDLr, and the highest in the validation set corresponds to CADD.

TABLE 2 Comparison of ESEA With Other ML Models

Model	Set	Sp	Sn	PPV	NPV	Technique
ESEA	Training	90.7	91.1	98.9	52.7	ESEA
	Validation	96.2	92.8	99.4	67.6	
LDA	Training	44.4	96.2	94.1	55.8	LDA
	Validation	50.0	95.1	92.4	61.9	
MLP 7:7-9-1:1 	Training	92.3	70.3	98.9	25.3	BP100, CG20, CG0b
	Validation	100	65.1	100	30.9	
RBF 4:4-9-1:1 	Training	90.7	66.1	98.5	22.5	KM, KN, PI
	Validation	92.3	66.3	98.2	30.0	
LNN 7:7-1:1 	Training	92.6	71.2	98.8	26.1	PI
	Validation	100	66.9	100	32.1	

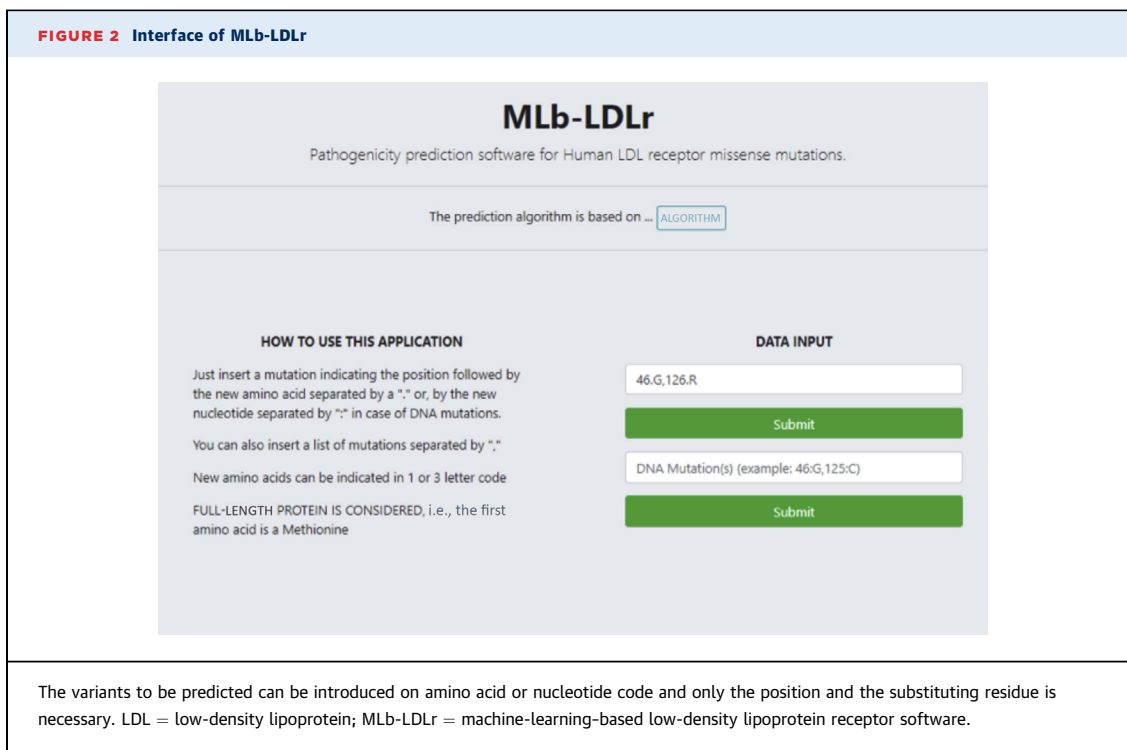
Green indicates positive input. Red indicates negative input.
 BP = backpropagation; CG = conjugated gradient; ESEA = Excel Solver Evolutionary algorithm; KM = K-means; KN = K-nearest neighbor; LDA = linear discriminant analysis; LNN = linear neural network; ML = machine learning; MLP = multilayer perceptron; NPV = negative predictive value; PI = pseudoinversion; PPV = positive predictive value; RBF = radial basis function; Sn = sensitivity; Sp = specificity.

These results are mostly maintained in bootstrapped samples, MutationTaster having the highest sensitivity values and CADD the highest specificity ones. MLb-LDLr on the other hand shows slightly lower values in most statistics because EGS optimization cannot be performed when bootstrapping samples.

Regarding area under the receiver operating curve (AUROC) values, CADD has the highest score (0.959) followed by MutationTaster (0.934), PolyPhen-2 (0.933), and MLb-LDLr (0.932).

As shown in Supplemental Table S11, 453 of 744 variants are correctly predicted by the 6 analyzed software programs, 181 variants are correctly predicted by 5 software programs, 62 variants are correctly predicted by 4 programs, 27 by 3 software programs, 17 by 2 software programs, and only 4 variants are correctly predicted by 1 or none. These results show that the 60% of the variants annotated in ClinVar are correctly predicted by any of the analyzed software programs, and that the remaining variants except for p.(Ala299Thr) can be correctly predicted by a combination of them. Altogether, this indicates that the available software should be used in combination to improve prediction accuracy.

IN VITRO FUNCTIONAL CHARACTERIZATION OF CONFLICTIVE *LDLr* VARIANTS. In order to experimentally validate the model, 13 *LDLr* variants were



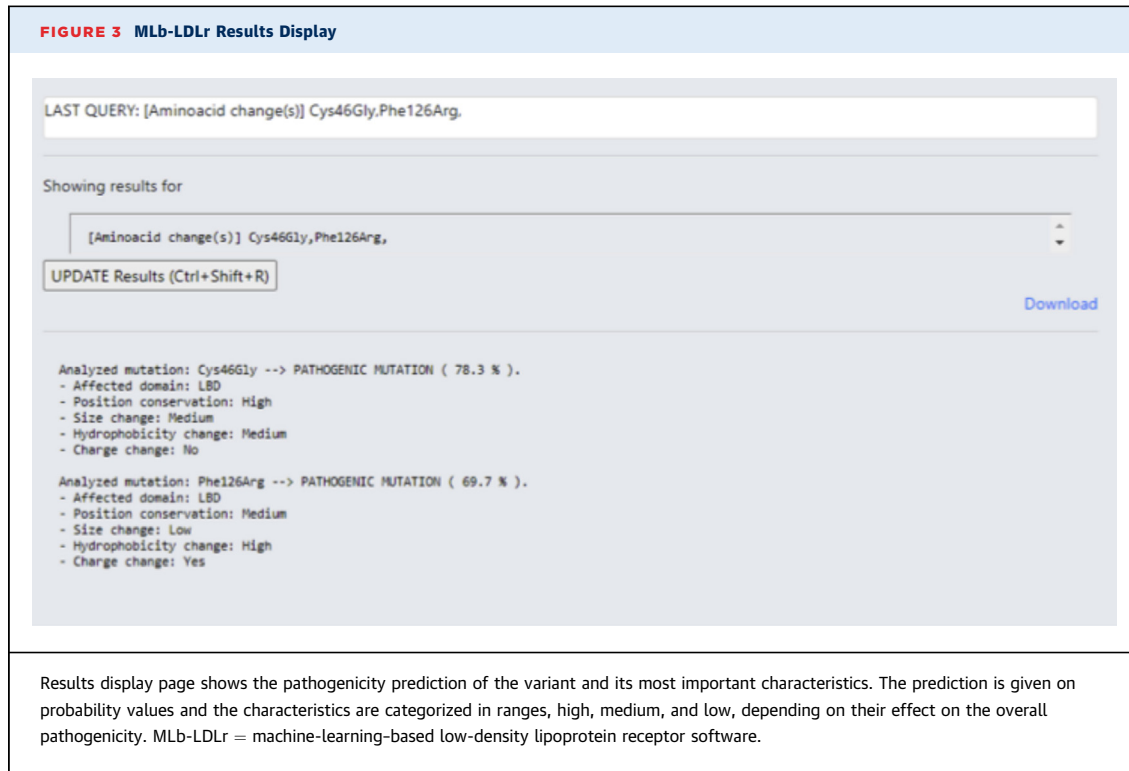
selected according to their conflictive interpretations in ClinVar and contradictive activity predictions. *LDLr* activity was assessed as indicated in Methods. As shown in [Figure 5](#), p.(Val578Ile) and p.(Pro683Leu) variants show similar *LDLr* activity to wild type, indicating that these mutations are not pathogenic. On the contrary, p.(Phe200Cys), p.(Asn297His), p.(Trp305Ser), p.(Lau371Pro), p.(Gly373Ala), p.(Arg449Gly), p.(Ile473Asn), p.(Asp638His), p.(Met652Thr), p.(Asp700Asn), and p.(Ala705Pro) variants showed a reduced activity ranging from 5% to 40% and thus are classified as pathogenic.

Activity results were compared with the pathogenicity predictions of each software program. As shown in [Table 4](#), MLb-LDLr shows the second-best accuracy for both pathogenic and benign variants, being the most balanced software. By contrast, PolyPhen-2 and CADD correctly predict barely more than one-half of the pathogenic variants and not a single benign variant. SIFT is the only one correctly predicting the benign variants, but only hits 2 pathogenic ones. MutationTaster correctly predicts 8 pathogenic variants, but no benign ones. Finally, SFIP-MutID has the highest score on pathogenic variants, but does not correctly predict any benign ones. The similarity between the results obtained in [Table 4](#)

and the prediction of the ClinVar database shown in [Table 3](#) is noteworthy.

DISCUSSION

Alongside the extraordinary growth of newly described *LDLr* variants brought by the fast development of next-generation sequencing (10), there is developing desire to develop powerful software to accurately assign biological activity roles to *LDLr* variants. PolyPhen-2, CADD, MutationTaster, and SIFT are some of the most used software packages to predict the effect of a mutation in the *LDLr* (18-21). PolyPhen-2 utilizes a combination of sequence-and structure-based attributes for the description of an amino acid substitution; SIFT makes inferences from sequence similarity; CADD is based on evulative gene factors and uses more than 60 variables; MutationTaster analyzes evolutionary conservation, splice-site changes, loss of protein features, and changes that might affect the amount of mRNA. Therefore, as they consider common features of many proteins, when predicting the effect on the activity of *LDLr* variants the results often disagree. More recently, a specific model for *LDLr* missense variants based on *LDLr* structural resolution has been



developed (SFIP-MutID), but the model lies in predicting pathogenic mutations rather than predicting benign mutations thus limiting its use (22).

This work sought to develop a ML model to improve accuracy on predicting the activity of missense *LDLr* mutations. It has previously been shown that combining information obtained from multiple sequence alignment and 3-dimensional protein structure can increase prediction performance (23). Therefore, specific features of the *LDLr* protein such as conservation of the substituted residue, charge change, the original amino acid, the substituting amino acid, hydrophobicity change, amino acid size change, and the location of the substituted amino acid within the different *LDLr* domains have been considered to quantify their influence on the overall pathogenicity. After having been represented as quantitative vectors, ESEA has been used to calculate both the weight of each characteristic on the overall pathogenicity and the threshold that determines whether a variant is pathogenic or not. The introduction of ClinVar database in the ML model constitutes an innovative feature about the MLb-LDLr software, which sets it apart from other software. This strategy allowed increasing the predictive power of the MLb-LDLr by integrating ML algorithms, resulting in a specificity of 92.5% and a

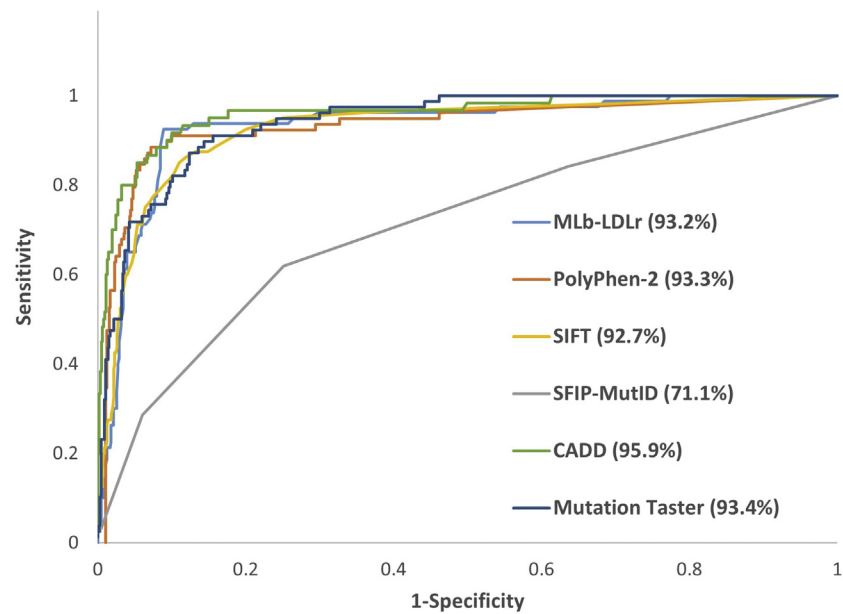
sensitivity of 91.6%. A major challenge in the MLb-LDLr optimization process was generating a balanced software program able to predict both pathogenic and benign variants with high accuracy. Our results demonstrated the value of combining information, especially the use of the ClinVar database, which provided predictive software with an accuracy higher than 90% in both pathogenic and benign variants.

The bootstrap resampling method is commonly used to test a model with many different training and

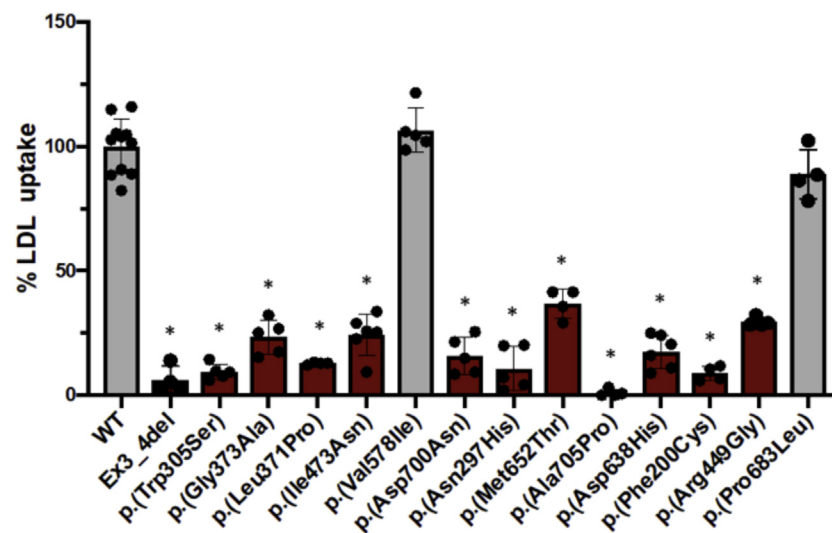
TABLE 3 Comparison of Predictive Software Using ClinVar Database

Predictive Tool	No Bootstrapping				Bootstrapping			
	T		V		T		V	
	Sn	Sp	Sn	Sp	Sn	Sp	Sn	Sp
MLb-LDLr ^a	90.7	91.1	92.8	96.2	87.5	91.2	85.8	81.8
PolyPhen-2	92.9	79.6	94.6	96.1	93.6	83.6	93.8	83.7
SIFT	83.9	90.7	90.3	88.5	85.4	89.9	85.5	90.5
SFIP-MutID ^b	92.1	18.5	87.3	26.9	90.5	21.1	90.5	21.1
CADD	88.5	88.9	89.7	100	88.9	92.5	89.1	92.6
MutationTaster	95.8	66.7	95.8	84.6	96.1	72.5	96.2	73.0

Statistics of the original sampling and randomly bootstrapped sampling. One thousand bootstrapped samples were used, and the results are shown with a 95% confidence interval. ^aThe expert-guided strategy optimization process cannot be carried out when bootstrapping, decreasing the accuracy of the model ^bSFIP-MutID is not able to predict mutation within 1-21 and 715-860 residues.
 T = training; V = validation; other abbreviations as in Tables 1 and 2.

FIGURE 4 Performance of MLb-LDLr in Comparison to Other Software

Several scores are compared by area under the receiver operating curve (AUROC) using the ClinVar database. MLb-LDLr = machine-learning-based low-density lipoprotein receptor software; other abbreviations as in [Tables 1 and 2](#).

FIGURE 5 In Vitro Validation of the Model by Assessing LDL Uptake on CHO-I Δ 7 Cells Transfected With *LDLr* Variants

LDL uptake was quantified by flow cytometry, as described in Methods. The values represent the mean of at least 4 experiments, error bars represent \pm SD. * $P < 0.01$ comparing WT with each variant. WT = wild-type; other abbreviations as in [Figure 2](#).

validation sets. This test is usually carried out automatically, because more than 1,000 groups are required, but the last process on MLb-LDLr software, EGS, must be done manually. Although the optimization process could not be implemented on the results shown in Table 3, these results are quite similar to the ones obtained with no EGS. Therefore, the bootstrapping resampling shows the validity of the training and validation set division, because the results obtained with and without bootstrapping are similar in all analyzed software programs.

All the analyzed software programs, except for CADD, provide pathogenicity predictions according to a specific threshold so that a probability value can be given as a result. By contrast, CADD is based on comparative scores and only provides relative pathogenicity values. This means that CADD relies on AUROC and similar general statistics to obtain an accuracy value; meanwhile, the rest of the software programs have optimized a specific threshold to obtain an optimum accuracy. This could explain why CADD has the highest AUROC values by far, but it is surpassed by MLb-LDLr and PolyPhen-2 on the overall accuracy.

SIFT and PolyPhen-2 are among the predictive software programs with the highest ease of use and speed, which allows for direct batch queries using amino acid and genome coordinates (24). In order to facilitate the use of MLb-LDLr, an interface has been developed, which allows direct input using DNA or amino acid nomenclature as well as querying multiple predictions.

One of the major advantages of MLb-LDLr software relies in the possibility of actualizing the dataset periodically thus including newly annotated variants in ClinVar. This allows continuously increasing database accuracy in order to perform an updated prediction for each new described variant. In the future, some other ML algorithms may be introduced in the MLb-LDLr software to integrate information such as phenotype of the patients carrying pathogenic variants and the most suitable treatment for each of them (25).

It is noteworthy that all the predicted models tested in this work showed an accuracy of over 80% when predicting variants, which indicates that the data accessible in ClinVar are highly accurate, even those with a single submitter to support the pathogenicity. This fact supports the use of the ClinVar database as a reliable source of information regarding pathogenic variants due to the big effort done to correctly assign pathogenicity to variants described

TABLE 4 Accuracy of MLb-LDLr, PolyPhen-2, SIFT, SFIP-MutID, CADD, and MutationTaster on 13 Characterized Novel *LDLr* Variants

Software	Predicted Pathogenic (n = 11)	Predicted Pathogenic, %	Predicted Benign (n = 2)	Predicted Benign, %	General Accuracy, %
MLb-LDLr	8	72	1	50	69
PolyPhen-2	6	54	0	0	46
SIFT	2	18	2	100	30
SFIP-MutID	10	91	0	0	77
CADD	6	54	0	0	46
MutationTaster	8	72	0	0	61

Values are n unless otherwise indicated.
 MLb-LDLr = machine-learning-based low-density lipoprotein receptor software; other abbreviations as in Tables 1 and 2.

so far. These pathogenic *LDLr* variants have been mostly found in patients with high plasma LDL plasma levels and have been characterized both by cascade screening or in vitro functional assays of the *LDLr* variants (10,26,27).

As mentioned in the preceding text, the fast development of next-generation sequencing brings to light a great number of new *LDLr* variants that will favor the emergence of benign ones. Hence, the development of predictive software such as MLb-LDLr with high accuracy in predicting benign variants is crucial. Nowadays, the simultaneous use of several software programs to predict the effect of a given mutation on protein activity is almost mandatory, because the ones with the highest accuracy on pathogenic variants have low accuracy on benign variants.

STUDY LIMITATIONS. First, MLb-LDLr software only predicts missense *LDLr* variants. There are many mutation types depending on their location and effect (frameshift, UTR, splicing site...), and each of them has a different mechanism that should be analyzed individually. Here, only missense variants have been analyzed because they represent a high percentage of total *LDLr* variants (40%) (8) and more than 50% in the ClinVar database (28,29). Although ClinVar is a great source to evaluate the pathogenicity of *LDLr* variants, 1 limitation of the database is that in some cases, there is only 1 submitter and a few of them have no assertion. In addition, there are enough cases of both missense pathogenic and benign variants to develop a ML model. Second, some P_{ik} values may not be totally correct due to the lack of enough benign variants in some classes. However, this problem will be fixed, because the number of characterized benign variants will increase. In the meantime, we tried to solve this by applying EGS strategy. The

accuracy of the artificial intelligence model using a validation cohort was not confirmed.

CONCLUSIONS

Here, we provide a powerful tool to predict the impact of *LDLr* mutations on protein activity. The strength of MLb-LDLr software relies in its precision with both type of variants, benign and pathogenic, with an estimated hit rate over 90% in both of them. These results highlight the usefulness of MLb-LDLr software as a helping diagnostic tool for clinicians.

ACKNOWLEDGEMENT The authors thank Mikel Larrea for his invaluable help in using some complex processes of Excel.

FUNDING SUPPORT AND AUTHOR DISCLOSURES

This study was supported by grants from the Basque Government (Cesar Martin, Grupos Consolidados IT-1264-19). Mr Larrea-Sebal was supported by a FPI grant from Gobierno Vasco (2019-2020). Dr Benito-Vicente was supported by Programa de especialización de Personal Investigador Doctor en la UPV/EHU (2019) 2019-2020. Dr Galicia-Garcia was supported by Fundación Biofísica Bizkaia. Ms Jebari-Benslaiman was supported by grant PIF (2017-2018), Gobierno Vasco. All other authors have reported that they have no relationships relevant to the contents of this paper to disclose.

ADDRESS FOR CORRESPONDENCE: Dr César Martín, Department of Biochemistry and Molecular Biology, Science and Technology School, University of the Basque Country (UPV/EHU), Barrio Sarriena s/n 48080 Bilbao, Spain. E-mail: cesar.martin@ehu.eus. OR Dr Humberto González-Díaz, IKERBASQUE, Basque Foundation for Science, Plaza Euskadi 5, 48011, Bilbao, Spain. E-mail: humberto.gonzalezdiaz@ehu.eus.

REFERENCES

1. Sjouke B, Kusters DM, Kindt I, et al. Homozygous autosomal dominant hypercholesterolaemia in the Netherlands: prevalence, genotype-phenotype relationship, and clinical outcome. *Eur Heart J*. 2015;36:560-565.
2. Brown MS, Goldstein JL. A receptor-mediated pathway for cholesterol homeostasis. *Science*. 1986;232(4746):34-47. <https://doi.org/10.1126/science.3513311>
3. Sharif M, Rakhit RD, Humphries SE, Nair D. Cardiovascular risk stratification in familial hypercholesterolaemia. *Heart*. 2016;102:1003-1008.
4. Ference BA, Ginsberg HN, Graham I, et al. Low-density lipoproteins cause atherosclerotic cardiovascular disease. 1. Evidence from genetic, epidemiologic, and clinical studies. A consensus statement from the European Atherosclerosis Society Consensus Panel. *Eur Heart J*. 2017;38:2459-2472.
5. Benito-Vicente A, Uribe KB, Jebari S, Galicia-Garcia U, Ostolaza H, Martin C. Familial hypercholesterolemia: the most frequent cholesterol metabolism disorder caused disease. *Int J Mol Sci*. 2018;19(11):3426.
6. Nordestgaard BG, Chapman MJ, Humphries SE, et al. Familial hypercholesterolaemia is underdiagnosed and undertreated in the general population: guidance for clinicians to prevent coronary heart disease. *Eur Heart J*. 2013;34:3478-3490.
7. Palacios L, Grandoso L, Cuevas N, et al. Molecular characterization of familial hypercholesterolemia in Spain. *Atherosclerosis*. 2012;221:137-142.
8. Chora JR, Medeiros AM, Alves AC, Bourbon M. Analysis of publicly available LDLR, APOB, and PCSK9 variants associated with familial hypercholesterolemia: application of ACMG guidelines and implications for familial hypercholesterolemia diagnosis. *Genet Med*. 2018;20:591-598.
9. Benito-Vicente A, Uribe KB, Jebari S, Galicia-Garcia U, Ostolaza H, Martin C. Validation of LDLr activity as a tool to improve genetic diagnosis of familial hypercholesterolemia: a retrospective on functional characterization of LDLr variants. *Int J Mol Sci*. 2018;19(6):1676.
10. Knowles JW, Rader DJ, Khoury MJ. Cascade screening for familial hypercholesterolemia and the use of genetic testing. *JAMA*. 2017;318:381-382.
11. Huijgen R, Kindt I, Defesche JC, Kastelein JJP. Cardiovascular risk in relation to functionality of sequence variants in the gene coding for the low-density lipoprotein receptor: a study among 29 365 individuals tested for 64 specific low-density lipoprotein-receptor sequence variants. *Eur Heart J*. 2012;33:2325-2330.

PERSPECTIVES

COMPETENCY IN MEDICAL KNOWLEDGE: This study developed a machine learning model (MLb-LDLr), which can help to provide a fast diagnosis to FH patients saving time and expenditure for characterizing the pathogenicity of *LDLr* variants. The MLb-LDLr software developed here can be clinically implemented to refine the diagnosis of FH and to improve disease prognosis. MLb-LDLr software may prove clinically useful and assist clinicians in tailoring precise management and therapy for the patients with FH and provide a novel diagnostic approach to manage FH. This study provides an open access predictive software to the scientific community, to predict the pathogenicity of missense *LDLr* variants.

TRANSLATIONAL OUTLOOK: The MLb-LDLr software increases the predictive power of previous software used to predict the pathogenicity of *LDLr* variants and provides an open-access interface to the scientific community and clinicians, which allows direct input using DNA or amino acid nomenclature as well as querying multiple predictions. The strength of MLb-LDLr software relies in its capacity of predicting both benign and pathogenic, with an estimated hit rate over 90%, highlighting the usefulness of MLb-LDLr software as a helping diagnostic tool for clinicians. Collectively, MLb-LDLr is expected to lower the incidence of cardiovascular events by collecting backpropagation data that are unmeasurable by current diagnostic modalities.

12. Wainberg M, Merico D, DeLong A, Frey BJ. Deep learning in biomedicine. *Nat Biotechnol*. 2018;36:829-838.
13. Thusberg J, Olatubosun A, Vihinen M. Performance of mutation pathogenicity prediction methods on missense variants. *Hum Mutat*. 2011;32:358-368.
14. MLb-LDLr software. Accessed September 30, 2021. <https://www.ehu.es/es/web/hypercholesterolemia-mechanisms/mlb-ldlr>
15. Barati R. Application of Excel solver for parameter estimation of the nonlinear Muskingum models. *KSCCE J Civ Eng*. 2013;17:1139-1148.
16. Galicia-Garcia U, Benito-Vicente A, Uribe KB, et al. Mutation type classification and pathogenicity assignment of sixteen missense variants located in the EGF-precursor homology domain of the LDLR. *Sci Rep*. 2020;10:1727.
17. Etxebarria A, Benito-Vicente A, Alves AC, Ostolaza H, Bourbon M, Martin C. Advantages and versatility of fluorescence-based methodology to characterize the functionality of LDLR and class mutation assignment. *PLoS One*. 2014;9(11):e112677.
18. Adzhubei IA, Schmidt S, Peshkin L, et al. A method and server for predicting damaging missense mutations. *Nat Methods*. 2010;7:248-249.
19. Sim NL, Kumar P, Hu J, Henikoff S, Schneider G, Ng PC. SIFT web server: predicting effects of amino acid substitutions on proteins. *Nucleic Acids Res*. 2012;40:452-457.
20. Rentzsch P, Witten D, Cooper GM, Shendure J, Kircher M. CADD: Predicting the deleteriousness of variants throughout the human genome. *Nucleic Acids Res*. 2019;47:D886-D894.
21. Schwarz JM, Rödelberger C, Schuelke M, Seelow D. MutationTaster evaluates disease-causing potential of sequence alterations. *Nat Methods*. 2010;7:575-576.
22. Guo J, Gao Y, Li X, et al. Systematic prediction of familial hypercholesterolemia caused by low-density lipoprotein receptor missense mutations. *Atherosclerosis*. 2019;281:1-8.
23. Berman HM, Battistuz T, Bhat TN, et al. The protein data bank. *Acta Crystallogr Sect D Biol Crystallogr*. 2002;58:899-907.
24. Dong C, Wei P, Jian X, et al. Comparison and integration of deleteriousness prediction methods for nonsynonymous SNVs in whole exome sequencing studies. *Hum Mol Genet*. 2015;24:2125-2137.
25. Sifrim A, Popovic D, Tranchevent LC, et al. EXTasy: variant prioritization by genomic data fusion. *Nat Methods*. 2013;10:1083-1086.
26. Etxebarria A, Benito-Vicente A, Palacios L, et al. Functional characterization and classification of frequent low-density lipoprotein receptor variants. *Hum Mutat*. 2015;36:129-141.
27. Lamiquiz-Moneo I, Civeira F, Mateo-Gallego R, et al. Diagnostic yield of sequencing familial hypercholesterolemia genes in individuals with primary hypercholesterolemia. *Rev Esp Cardiol (Engl Ed)*. 2021;74(8):664-673.
28. Harrison SM, Riggs ER, Maglott DR, et al. Using ClinVar as a resource to support variant interpretation. *Curr Protoc Hum Genet*. 2016;89:8.16.1-8.16.23.
29. Landrum MJ, Lee JM, Benson M, et al. ClinVar: improving access to variant interpretations and supporting evidence. *Nucleic Acids Res*. 2018;46:D1062-D1067.

KEY WORDS familial hypercholesterolemia, LDL receptor, machine learning software, pathogenicity, prediction

APPENDIX For an expanded Methods section as well as supplemental tables, please see the online version of this paper.